Performance analysis of UHF mobile satellite communication system experiencing ionospheric scintillation and terrestrial multipath fading

Paulo Victor R. Ferreira and Alexander M. Wyglinski
Wireless Innovation Laboratory
Department of Electrical and Computer Engineering
Worcester Polytechnic Institute, Worcester, MA, USA
{prferreira, alexw}@wpi.edu

***Abstract*—This paper analyzes a mobile satellite communication system with respect to the BER performance between a geostationary satellite and a moving node. Specifically, we study a scenario where the channel causes ionospheric scintillation-based multipath fading within the UHF frequency band. The scenario considers medium and high ionospheric scintillation indexes for Rural Area (RA) and Hilly Terrain (HT) multipath profiles. A BER performance decrease of more than 2 orders of magnitude for an ionospheric scintillation index of 0.3 occurs when the terrestrial multipath fading is added to ionospheric scintillated signals. This effect can be associated with satellite link loss, such as the one observed during Operation Anaconda at the Battle of Takur Ghar [1] in Afghanistan. Consequently, we propose a channel model that accounts for these effects, composed by two Rician channels connected in series and employs a K-factor equation in terms of the terrain's reflection coefficient.**

***Index Terms*—Satellite communication, multipath fading, ionospheric scintillation, mobile communications, terrestrial multipath, Rician channel model**

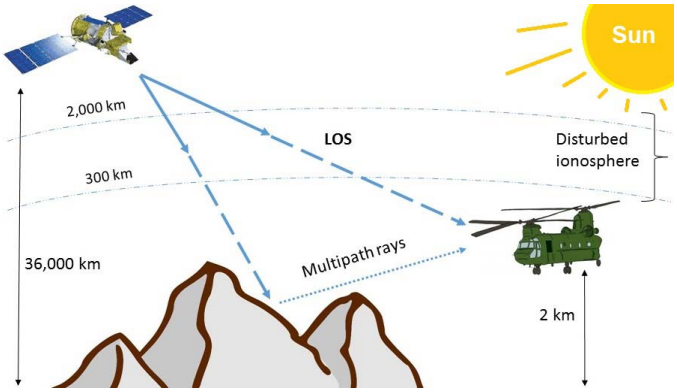

Fig. 1. Illustration of a communication link between a mobile node and a GEO satellite. The received signal is a combination of the scintillated LOS and multiple reflections of scintillated rays.

I. Introduction

During a military operation in Afghanistan called Operation Anaconda, which occurred during the peak of Solar Cycle 23 (March 2002), a message sent to NATO forces alerting them to avoid the Takur Ghar mountain via a geostationary (GEO) UHF satellite was never received [1]. Often UHF satellite communications employ carrier frequencies around 250 MHz, and according to [1] the elevation angle from the Takur Ghar region to the UFO-10 satellite was approximately 52°. Frequencies under 3 GHz are often susceptible to ionospheric fast fading, known as ionospheric scintillation [2], for specific elevation angles, link margins, ground station latitudes, and specific times of day, although higher frequencies may also be susceptible.

Based on several public accounts of the operation [3], [4], it was observed that communications were not reliable during this time period and that a number of recent scientific studies [1] have identified space weather as one of the main contributors for the communication link disruption during the military operation. These studies also mentioned that the space weather effects were enhanced by the multipath fading caused by the terrain, but did not quantify their combined effect.

In order to disrupt a satellite communication link, the event causing the fading does not need to persist for a long time duration. Rather, it just needs to occur across a certain period of time with a high intensity, which is the typical behavior of ionospheric scintillation. Given that most robust satellite communication systems use some sort of network protocol, if the fading event occurs during an exchange of synchronization messages between a transmitter and a receiver, the link can no longer be sustained and a transmission disruption occurs.

When such a fading event occurs for a receiver moving over terrain such as mountains, flat ground, or over the sea, the multipath contribution of the scintillated signals may either be constructive or destructive. If the latter occurs during the same period of the communication protocol when synchronization messages are exchanged, the fading effect is enhanced and a link disruption occurs. The scenario when the multipath fading of scintillated signals occurs is depicted in Fig. 1.

Previous studies have developed analytical mobile satellite channel models that combine ionospheric scintillation and terrestrial multipath [5]–[8]. However, these studies have omitted

This work was supported in part by the Brazilian Federal Agency for the Support and Evaluation of Graduate Education (CAPES) through the Science without Borders scholarship program.

978-1-4799-8091-8/15/$31.00 ©2015 IEEE

the terrain's reflection coefficient from within the Rician factor. Furthermore, these studies did not explicitly show the digital communications system performance in terms of BER.

In this paper we propose a channel model that builds upon the current state-of-the-art and includes the Rician K-factor in terms of the reflection coefficient, considering the Doppler delay spectrum and terrain profiles recommended by COST 207 [9] for the terrestrial multipath fading. The proposed channel model is composed of two Rician channels connected in series. The multipath fading K-factor equation is derived in terms of the terrain's reflection coefficient. The BER analysis is performed for scenarios using different terrain profiles under different ionospheric conditions.

The rest of this paper is organized as follows: In Section II, we give an overview on how the trans-ionospheric signals are affected by space weather as well as by the multipath fading channel considered. In Section III, we describe the simulation testbed and the parameters used. We also discuss the results achieved. In Section IV, we wrap up our conclusions and point out future work and next steps.

II. Mobile Satellite Communications Channel impairments

In mobile satellite communications, there are several factors that contribute to the total signal attenuation. The most significant factor is the free-space loss due to the decrease in power density between a node on the ground and a GEO satellite. In this paper, we consider that such loss is recovered by the receiver amplifiers and that we are interested in attenuation sources other than the free-space loss. We also assume that the moving node has a constant speed of 250 km/h (70 m/sec) at a constant altitude of 2 km. Furthermore, we focus on two other attenuation sources depicted in Fig. 1: ionospheric scintillation and terrestrial multipath fading. We point out that even though there can be fading on both uplink and downlink, the analysis and simulations done in this paper are for only the downlink.

A. Ionospheric scintillation

The ionosphere is a region in the Earth's atmosphere located between 200 km to $2,000$ km in altitude [10], [11]. It is primarily characterized by the presence of ionized gas, *i.e.*, plasma. The ionization within this region occurs by the photo-ionization process as a result of two main events: the daily illumination by the Sun and sporadic Sun disturbance events, such as solar flares or geomagnetic storms [12]–[14].

The first event repeats every day, with the ionization intensity of the upper layers of the ionosphere varying throughout the day. This event is more intense at latitudes between $\pm$ 40 degrees [11] around the Equator. Just after the local sunset, the recombination of electrons begin. However, this process is not uniform throughout a column of the ionosphere with a certain height. Thus, non-uniform density ion regions start to build up during the night, known as ionospheric bubbles, at scales ranging from a few centimeters up to tens of kilometers. This recombination event usually occurs during a daily local time window starting at 20:00 local time and lasting up to local midnight.

Space weather is another factor that can enhance the ionization or cause ionospheric disturbances during anytime of day [15]. It also has the potential to extend the disturbance up to higher latitudes. The space weather activity period tends to follow the 11 years solar cycle according to the sunspot number [13]. Depending on the intensity of the solar event, disruptions to satellite communication links can occur if the Earth is in view of the Sun sector where the event occurred [16].

The power of an electromagnetic field traveling through a ionospheric disturbance ionosphere varies very quick. This fading effect is called ionospheric scintillation [10], and its intensity is function of the current ionospheric density gradient faced by the traveling signal.

B. Multipath fading

The scenario shown in Fig. 1 demonstrates the importance of the terrain over which the mobile node is moving. Depending on the terrain landscape and the electrical properties of its material, the incident rays will be reflected with different intensities and phases.

In our case, there is no signal shadowing and the Line of Sight (LOS) signal component is always present. Also, for the case where the receive antenna is located far from the scatters, the LOS power can be considered larger than the power of the multipath rays. The result of these reflected rays combine either constructively or destructively, with the LOS component at the receive antenna. In this paper, both LOS and reflected rays are scintillated rays reflected by the terrain profiles considered.

III. Proposed channel model

Several measurement campaigns assessed the intensity ionospheric scintillations within the L-band for GPS systems [2], [10], [17]. Based on these measurements, statistical models have been proposed, with the Rician [18], [19] and Butterworth 2^{nd} order filter [19] models being widely accepted. The recommended approach is to model the scintillation channel using a Butterworth filter since it relies heavily on measurements for defining fading intervals, *i.e.*, the 3 dB autocorrelation time-lag, for different frequency bands [18]. However, in the literature there is a lack of such measurements for the scintillation at satellite communications for nodes traveling more than 125 mph over different terrain profiles. Thus, we use a Rician channel model, which has the probability density function [19]:

$$p(\alpha) = \frac{2\alpha(1+K)}{\Omega} I_0\left(2\alpha\sqrt{\frac{K+K^2}{\Omega}}\right) e^{\frac{-K-\alpha^2(1+K)}{\Omega}}, \quad (1)$$

where K is the Rician factor, the variable α is the magnitude of the complex channel response function, it is normalized, $\alpha \geq 0$, and has a second moment, *i.e.*, mean-square for the fading amplitude $\Omega \equiv \ E[\alpha^2] = 1$.

The scintillation index S_4 is defined by the squared-root of the normalized variance of the signal intensity I over a given interval of time, usually is 1 minute with a measurement sample rate of 1 Hz, defined by:

$$S_4 = \sqrt{\frac{E[I^2] - E[I]^2}{E[I]^2}}. \quad (2)$$

The Rician parameter K is related to S_4 by [19]:

$$K = \frac{\sqrt{1 - S_4^2}}{1 - \sqrt{1 - S_4^2}}, 0 \leq \ S_4 \ \leq \ 1. \quad (3)$$

The multipath model has a Rician distribution with different parameters from the Rician distribution of the scintillation model. We derive a K-factor that is a function of the reflection coefficient Γ, which in turn is a function of the carrier frequency f, incidence angle θ_i, reflection angle θ_0, and the electrical properties of the terrain's material, such as relative permittivity ε_r and conductivity σ. The approach taken is to define a Rician K-factor function of the reflection coefficient by using the classical two-ray propagation model [20], assuming that $\theta_i = \theta_0 = \theta$, where θ is the satellite elevation angle.

The reflection coefficient Γ is given by [21]:

$$\Gamma = \frac{Csin\theta - \sqrt{(\varepsilon_r - j\chi) - (cos\theta)^2}}{Csin\theta + \sqrt{(\varepsilon_r - j\chi) - (cos\theta)^2}}, \quad (4)$$

where $C = \varepsilon_r - j\chi$ for vertical polarization and $C = 1$ for horizontal polarization. Furthermore, χ is given by:

$$\chi = \frac{\sigma}{\omega\varepsilon_0} = \frac{\sigma}{2 \ \pi \ f \ \varepsilon_0} = \frac{1.8 \times \ 10^{10}\sigma}{f}, \quad (5)$$

with $\varepsilon_0 = 8.854 \times \ 10^{-12}$ F/m. The phase difference between the two reflected paths is given by [20]:

$$\Delta\phi = \frac{2\pi}{\lambda}\left(\sqrt{d^2 + (h_t + h_r)^2} - \sqrt{d^2 + (h_t - h_r)^2}\right), \quad (6)$$

where λ is the wavelength, d is the distance between the transmitter and receiver antennas, h_t and h_r are the height of the transmitter and receiver antennas, respectively.

The resultant received power p_r is given by the sum of the LOS received power plus the received multipath power, resulting in:

$$p_r = p_t\left(\frac{\lambda}{4 \ \pi \ d}\right)^2 G_t G_r[1 + |\Gamma|^2 + 2|\Gamma|cos(\angle\Gamma - \angle\Delta\phi)], \quad (7)$$

which is function of transmitter power p_t and the reflection coefficient [21], where G_t and G_r are the transmitter and receiver antenna gains, respectively.

Since the K-factor is defined as the ratio of the LOS power to the multipath power, the former cancels out, resulting in:

$$K = \frac{1}{|\Gamma|^2 + 2|\Gamma|cos(\angle\Gamma - \angle\Delta\phi)}. \quad (8)$$

It is worth noting that for the geometry considered in our case, the elevation angle is assumed constant for the area where the mobile node is moving around. For longer distances, one might consider θ to be function of time, as well as if the satellite is in Low-Earth orbit (LEO).

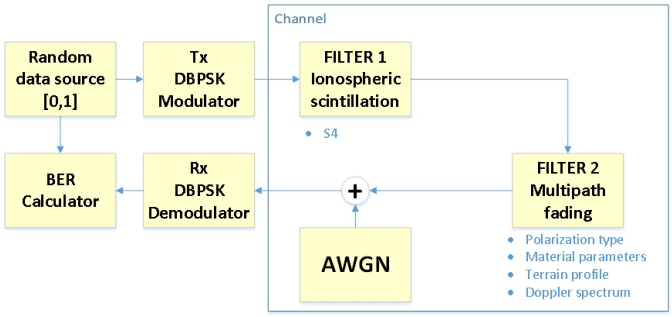

Fig. 2. Schematic of the mobile satellite communication system simulation testbed implemented in MATLAB. Two Rician channels model the effects of ionospheric scintillation and multipath fading.

The nature of our scenario, consisting of a mobile node, suggests that the propagation delay is long [9], [22], in which case we can use a "Gaussian I" type for the Doppler power spectrum, suitable for multipath components with long delays in UHF communications [23], which is also proposed as a model for the aeronautical satellite channel [24], [25]. For this Doppler spectrum, the propagation delay τ has an interval $0.5 \ \mu s \ \leq \ \tau \ \leq \ 2 \ \mu s$ with a Doppler spread given by $\sigma = 0.45 f_{max}$, where $f_{max} = \frac{vf}{c}$ is the maximum Doppler frequency [9], [22], where v is the node linear speed in m/s, f is the carrier frequency in Hz, and c is the speed of light in m/s. For the Gaussian I Doppler power spectrum, the standard deviation σ_N normalized by f_{max} is $\sigma_N = \frac{\sigma}{f_{max}} = 0.45$.

IV. Simulation Results

The simulation testbed used in this work was implemented in MATLAB [26] and is composed of a transmitter, a channel, and a receiver. Fig. 2 shows the diagram block of the simulation testbed. Based on the discussion about the channel parameters in the previous section, the implementation of the two main channel impairments, scintillation and multipath, uses Rician channel models, each with different parameters, and the Additive White Gaussian Noise (AWGN) channel representing the noise at the receiver.

For this experiment, random bits are modulated using a DBPSK modulation scheme and sent through the channel to the receiver. The ionospheric channel input is the S_4 index. The multipath channel inputs are: polarization type, material parameters, terrain profile and Doppler power spectrum density distribution. The simulations were performed for all the combinations of parameters shown in Table I.

The values used for the electrical material properties can be found in Table 4.1 in [20]. The $\mathcal{L}$-path channel model models containing the propagation delay in seconds and the path power in dB for each of the terrain profiles described in Table I follow the COST 207 [9] recommendations and can be found in Table 7.2 in [22].

TABLE I
SIMULATION PARAMETERS TO BE COMBINED INTO 4 DIFFERENT SCENARIOS

S_4	Frequency	Polarization	Terrain profile	Material
Medium $S_4 = 0.3$	UHF (250 MHz)	Horizontal	Rural Area (RA)	Poor Ground
High $S_4 = 0.9$		Vertical	Hilly Terrain (HT)	

Following, the noise is added to the signal using the AWGN channel, which had its $\frac{E_b}{N_0}$ parameters varied from 0 dB to 20 dB at 2 dB step for the BER curve acquisition. Then, $20,000$ symbols were transmitted per frame with a total of 100 runs for each $\frac{E_b}{N_0}$ value, such that the minimum value for bit error for each $\frac{E_b}{N_0}$ was guaranteed to be 100. The maximum Doppler shift considered was 60 Hz for a node moving at 70 m/sec and a carrier frequency of 250 MHz. Then, the Doppler spread is $\sigma = 0.45 f_{max} = 27$ Hz. Since $\sigma \ll f_{max}$, the channel is expected to be slow fading. Two S_4 indexes were considered: $S_4 = 0.3$ for medium scintillation and $S_4 = 0.9$ for high scintillation. Even though the considered satellite uses circular polarization, simulations were performed for two different polarizations: horizontal and vertical. Thus, the following results are bounds on BER performance, not precise estimates. Two terrain profiles were considered for the path gains and delay profiles: 4-path Rural Area (RA) and 6-path Hilly Terrain (HT) channel models [22].

For the reflection coefficient of the K-factor for Filter 2 in Fig. 2, which uses the two-ray model, the antenna heights considered as shown in Fig. 1 are $36,000$ km and 2 km for the satellite and mobile node, respectively. The range between the two antennas is $36,497$ km and was computed using the STK software by AGI [27] for the Takur Ghar region ($33°20'35''N,\ 69°12'52''E$) to the UFO-10 satellite ($77.5°\ E$).

The material parameters are defined in terms of their material electrical properties. It was considered a Poor Ground material type with relative permittivity $\varepsilon_r = 4$ and conductivity $\sigma = 0.001$ [20]. Regarding the terrain profiles, the values used for the path gain and propagation delay were taken from the COST 207 [9] recommendation. The K-factors for the scenarios considered are described in Table II. Since the terrain material, frequency, and antenna distances were constant for this experiment, the K-factor changes with the polarization type only, but is function of all these parameters.

TABLE II
RICIAN K-FACTORS FOR IONOSPHERIC SCINTILLATION AND TERRESTRIAL MULTIPATH FADING FILTERS

Filter 1		Filter 2	
Parameter	K-factor	Parameters	K-factor
Medium $S_4 = 0.3$	20.7104	Horizontal pol.	6.2943
High $S_4 = 0.9$	0.7727	Vertical pol.	16.6698

After running the simulations for the combinations of channel parameters in Table I, the results are split in terms of terrain profile and polarization. For a performance reference, the BER for the link using only the AWGN channel is given. Next, results were obtained by adding Filter 1 in order to analyze the effect of simulated ionospheric scintillation. The Filter 2 was connected in series with Filter 1, allowing for the analysis of terrestrial multipath fading of ionospheric scintillated signals. The results for RA and HT terrain profiles are shown in Fig. 3 and Fig. 4, respectively. Both figures show distinct left and right panels for the simulations using horizontal and vertical polarization, respectively.

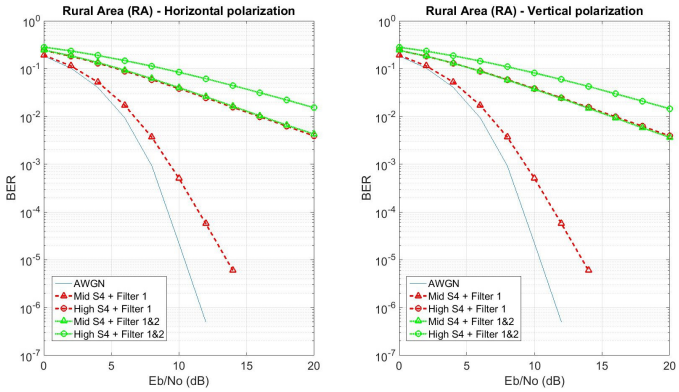

Fig. 3. BER performance of mobile communication link for a Rural Area (RA) 4-path channel model under ionospheric scintillation. Left panel shows results for horizontal polarization and right panel shows results for vertical polarization.

From Fig. 3, it is clear that the BER performance difference between polarizations are minimal given the scenario assumptions as well as transmitter and receiver configurations. Furthermore, the BER performances for a scenario with high S_4 using only Filter 1 and the scenario with medium S_4 using Filters 1 and 2 are similar. Both panels in Fig. 3 show a great decrease in BER performance for medium S_4 while comparing a scenario with only scintillation and another with multipath of scintillated signals (dashed and dotted lines with triangle markers, respectively). This decrease is more than two orders of magnitude for $\frac{E_b}{N_0} = 12$ dB. For high S_4, the BER performance is worse as expected. However, the decrease in performance in this last case is smaller, less than one order of magnitude over the entire range of $\frac{E_b}{N_0}$ simulated.

From Fig. 4, it is also observed minimal BER performance differences between the two polarizations. As expected, the overall BER performance for the two polarizations in the HT terrain profile are worse than the performances in the RA profile. The main performance difference between the profiles are for the multipath fading of ionospheric scintillated signals,

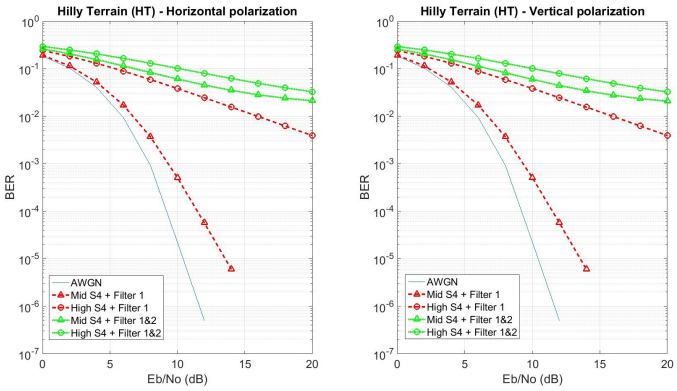

Fig. 4. BER performance of mobile communication link for a Hilly Terrain (HT) 6-path channel model under ionospheric scintillation. Left panel shows results for horizontal polarization and right panel shows results for vertical polarization.

from 3×10^{-2} to 1.5×10^{-2} for medium S_4 and from 2×10^{-2} to 3×10^{-3} for high S_4, both for $\frac{E_b}{N_0} = 20\ dB$.

V. Conclusions

This paper aimed to analyze the BER performance of a mobile satellite communication system between a GEO satellite and a moving node under multipath fading of scintillated signals while traveling through different terrain profiles under different scintillation indexes. In order to implement the channel, a model composed of two Rician channels connected in series was proposed. Furthermore, the K-factor in terms of the terrain's reflection coefficient was derived for the Rician channel implementing the multipath fading.

Simulations for Rural Area (RA) and Hilly Terrain (HT) profiles were performed. We also analyzed the performance for horizontal and vertical polarization. As expected, the performance for the HT profile was found to be worse than the RA profile.

The root cause assumed in [1] alone does not seem to justify the possible message delivery failure based on the results shown by Fig. 4, which assumes the scenario parameters and conditions close to the mountain region. Depending on the polarization type used, the BER performance can be even worse depending on the $\frac{E_b}{N_0}$ being used. Thus, we showed that there is a significant BER performance decrease when the communicating node changes from a scenario where only ionospheric scintillation is present, such as a node flying at high altitudes, to another where there is multipath fading of ionospheric scintillated signals, with the performance decrease reaching some orders of magnitude depending on the $\frac{E_b}{N_0}$ being used.

References

[1] M. A. Kelly and et. al., "Progress toward forecasting of space weather effects on UHF satcom after Operation Anaconda," *American Geophysical Union*, 2014.

[2] "Rec. ITU-R P.531-12 - Ionospheric propagation data and prediction methods required for the design of satellite services and systems," International Telecommunication Union, Tech. Rep., 2013.

[3] S. Naylor, *Not a Good Day to Die: The Untold Story of Operation Anaconda*. Berkley Hardcover, 2005.

[4] L. Neville, *Takur Ghar-the SEALs and Rangers on Roberts Ridge Afghanistan 2002*. Osprey, 2013.

[5] Z. Ye and E. Satorius, "Channel modeling and simulation for mobile user objective systems - part I: Flat scintillation and fading," *Proceedings of IEEE International Conference on Communications*, 2003.

[6] ——, "Channel modeling and simulation for mobile user objective systems - part II: Selective scintillation and terrestrial multipath fading," *Proceedings of IEEE International Conference on Communications*, 2003.

[7] R. Kumar, "Scaterring functions for fading channels with ionospheric scintillation and terrestrial multipath," *IEEE Aerospace Conference Proceedings*, 2005.

[8] J. Hant and et. al., "Verification of satellite-channel simulator with scintillation, terrestrial multipath and shadowing effects," *Proceedings of IEEE Aerospace Conference*, 2005.

[9] M. Failli, "COST 207: Digital Land Mobile Radio Communications," Luxembourg: Commission of the European Communities, Tech. Rep., 1989.

[10] M. C. Kelley, *The Earths Ionosphere. Plasma Physics and Electrodynamics*. Academic Press, 1989.

[11] J. Huba and G. Joyce, "Global modeling of equatorial plasma bubbles," *Geophysical Research Letters*, 2010.

[12] "National Aeronautics and Space Administration," National Aeronautics and Space Administration. [Online]. Available: http://www.nasa.gov

[13] "National Oceanic and Atmospheric Administration satellite information system," National Oceanic and Atmospheric Administration. [Online]. Available: http://www.noaasis.noaa.gov/NOAASIS/ml/genlsatl.html

[14] "About ionospheric scintillation," Australian Government Bureau of Meteorology. [Online]. Available: http://www.ips.gov.au/Satellite/6/3

[15] "Sun unleashes 1st monster solar flare of 2015," Space.com. [Online]. Available: http://www.space.com/28797-sun-unleashes-monster-solar-flare-x2.html

[16] "Severe solar storm hitting earth," USA Today. [Online]. Available: http://www.usatoday.com/story/weather/2015/03/17/solar-geomagnetic-storm/24901903/

[17] "Embrace," Instituto Nacional de Pesquisas Espaciais. [Online]. Available: http://www2.inpe.br/climaespacial/portal/sci-home/

[18] Y. Feria and et. al., "Solar scintillation effects on telecommunication links at Ka-Band and X-Band." *TDA Progress Report 42-129*, May 1997.

[19] T. Humphreys and et. al., "Simulating ionosphere-induced scintillation for testing gps receiver phase tracking loops," *IEEE Journal of Selected Topics in Signal Processing*, 2009.

[20] T. S. Rappaport, *Wireless Communications Principles and Systems*. Prentice-Hall, 2002.

[21] E. C. Jordan and K. G. Balmain, *Electromagnetic Waves and Radiating Systems*. Prentice-Hall, 1968.

[22] M. Patzold, *Mobile Radio Channels*. Prentice-Hall, 2002.

[23] D. C. Cox, "Delay doppler characteristics of multipath propagation at 910 MHz in a suburban mobile radio environment," *IEEE Transactions on Antennas and Propagation*, 1972.

[24] P. A. Bello, "Aeronautical channel characterizations," *IEEE Transactions on Communications*, 1973.

[25] A. Neul and et. al., "Aeronautical channel characterization based on measurement flights," *Proceedings IEEE Global Communications Conference*, 1987.

[26] MATLAB, *version 8.2.0.701 (R2013b)*. Natick, Massachusetts: The MathWorks Inc., 2013.

[27] STK, *version 10.1.0*. Exton, PA: Analytical Graphs, Inc., 2014.